Published in final edited form as:
Neurobiol Dis. 2010 November ; 40(2): 432–443. doi:10.1016/j.nbd.2010.07.003.

Aspartoacylase deficiency affects early postnatal development of oligodendrocytes and myelination

Natalia S. Mattan[a,c], **Cristina A. Ghiani**[b,c], **Marcia Lloyd**[a,d], **Reuben Matalon**[e], **Dean Bok**[a,d], **Patrizia Casaccia**[f], and **Jean de Vellis**[a,b,c,*]

[a] Department of Neurobiology, David Geffen School of Medicine, University of California Los Angeles, Los Angeles, CA 90095, USA

[b] Department of Psychiatry, David Geffen School of Medicine, University of California Los Angeles, Los Angeles, CA 90095, USA

[c] Intellectual and Developmental Disabilities Research Center, David Geffen School of Medicine, University of California Los Angeles, Los Angeles, CA 90095, USA

[d] Jules Stein Eye Institute, David Geffen School of Medicine, University of California Los Angeles, Los Angeles, CA 90095, USA

[e] Department of Pediatrics, The University of Texas Medical Branch, Galveston, TX 77555, USA

[f] Departments of Neuroscience and Genetics and Genomics, Mount Sinai School of Medicine, New York, NY 10029, USA

Abstract

Canavan disease (CD) is a neurodegenerative disease, caused by a deficiency in the enzyme aspartoacylase (ASPA). This enzyme has been localized to oligodendrocytes; however, it is still undefined how ASPA deficiency affects oligodendrocyte development. In normal mice the pattern of ASPA expression coincides with oligodendrocyte maturation. Therefore, postnatal oligodendrocyte maturation was analyzed in ASPA-deficient mice (CD mice). Early in development, CD mice brains showed decreased expression of neural cell markers that was later compensated. In addition, the levels of myelin proteins were decreased along with abnormal myelination in CD mice compared to wild-type (WT). These defects were associated with increased global levels of acetylated histone H3, decreased chromatin compaction and increased GFAP protein, a marker for astrogliosis. Together, these findings strongly suggest that, early in postnatal development, ASPA deficiency affects oligodendrocyte maturation and myelination.

Keywords

Oligodendrocytes; Neural cells; Development; Canavan disease; Aspartoacylase; Leukodystrophy

Introduction

Canavan disease (CD) is a devastating neurodegenerative disease, characterized by developmental delays and mental retardation (Matalon et al., 1995). CD patients display degeneration of the white matter, demyelination and, as shown by histological analysis, a spongy brain appearance. These effects are caused by a recessive mutation in the aspartoacylase

*Corresponding author. UCLA-Intellectual and Developmental Disabilities Research Center, 635 Charles E Young Drive South, Los Angeles, CA 90095-7332, USA. Fax: +1 310 206 5061. jdevellis@mednet.ucla.edu (J. de Vellis).

(ASPA)-encoding gene (Adachi et al., 1973; Matalon et al., 1988; de Coo et al., 1991). ASPA is an enzyme reported to be involved in the hydrolysis of N-acetyl-aspartate (NAA) into acetate and aspartate (Kaul et al., 1991; Moffett et al., 2007). CD is therefore characterized by a dramatic increase in NAA levels and a decrease in the products acetate and aspartate (Hagenfeldt et al., 1987; Bluml, 1999; Kumar et al., 2006). Early observations suggested an association of CD with oligodendrocytes due to loss of white matter as a result of the absence of functional ASPA (Kaul et al., 1991). ASPA mRNA was localized to the white matter of postnatal rats (Kirmani et al., 2003) and mice (Kumar et al., 2009), in oligodendrocytes (Baslow, 1999; Bhakoo and Pearce, 2000; Bhakoo et al., 2001; Kirmani et al., 2003; Klugmann et al., 2003; Madhavarao et al., 2004), and also in purified myelin (Wang et al., 2007), thereby suggesting the potential involvement of ASPA in oligodendrocyte development. Furthermore, numerous studies have implicated the role of hydrolyzed NAA in supplying acetyl groups for lipid synthesis, an important component of myelin (D'Adamo et al., 1968; Burri et al., 1991; Miller, 1996; Chakraborty et al., 2001). It is believed that NAA plays an important role and serves as a type of neuronal support in myelin formation (Chakraborty and Ledeen, 2003; Wang et al., 2009). In addition, a decrease in the synthesis of myelin-associated lipids and reduced acetate levels have been reported during myelination in CD mice (Madhavarao et al., 2005), suggestive of altered lipid synthesis (Ledeen et al., 2006; Namboodiri et al., 2006), and of a significant role of ASPA in oligodendrocyte maturation. Besides the role in myelin formation and function, acetylation also modulates the function of nucleosomal histones, chromatin components that have been shown to play a critical role in the expression of genes important for oligodendrocyte maturation (Liu and Casaccia, 2010). Based on these premises, we hypothesized that ASPA could play a critical role in oligodendrocyte development and contribute to CD pathophysiology.

Since CD is a childhood disease, a study of oligodendrocytes and their development during the early stages of disease pathogenesis is crucial to better understand the underlying mechanisms of disease progression.

In the present study, in order to better understand the role of ASPA in oligodendrocyte maturation we investigated early postnatal development in a mouse model of CD, which carries a mutation in the ASPA gene causing a defect in enzyme activity (Matalon et al., 2000).

Materials and methods

Animals

Animals were obtained from R. Matalon (Galveston, TX) and housed at UCLA, in a controlled facility, with a temperature of 37 °C, under a light/dark cycle and food *ad libitum*. Mouse genotypes were confirmed by tail clipping and PCR using the following primers: ASPA (F-TTTTAACGCTTAATTTTCTCAACA, R-TTGGTTAAGTTTTGCACAGACC), and ASPA F with IRES (R-AGGAACTGCTTCCTTCACGA), yielding a fragment of 257 bp for $ASPA^{+/+}$ and 457 bp for $ASPA^{-/-}$ mice, respectively. $ASPA^{+/-}$ mice showed both fragments. DNA was isolated using Genscript TissueDirect Multiplex System (Genscript Corporation, Piscataway, NJ) and amplified using the GeneAmp PCR Reagent Kit (Applied Biosystems, Foster City, CA). Mice were sacrificed at different ages (P1, 7, 15, 20, 30, and 60), and 3–4 wild-type (WT) or CD mice were used for each time point, and were analyzed in 3–4 independent experiments. The studies were performed in accordance with the NIH guidelines for the Care and Use of Laboratory Animals, and approved by the UCLA Chancellor's Animal Research Committee.

Immunohistochemistry

Animals were anesthetized and perfused intracardially with 4% paraformaldehyde (PFA) in 1× PBS. The brain was removed, post-fixed overnight in 4% PFA at 4 °C, cryopreserved in 15% sucrose and embedded in Tissue Tek OCT compound. Frozen sections were cut at 12 μm. When sections were used, they were blocked in carrier solution (1% bovine serum albumin +0.3% Triton-X100 in PBS) containing 20% normal goat serum (NGS) for 1 h, followed by an overnight incubation with primary antibody at 4 °C in carrier solution containing 5% NGS. Sections were incubated with the appropriate secondary antibodies conjugated to Cy3 (Jackson ImmunoResearch Laboratories Inc., West Grove, PA) or Alexa Fluor® 488 (Molecular Probes, Eugene, OR) and then mounted in Vectashield mounting medium with DAPI (Vector Laboratories, Burlingame, CA). Immunostained sections were analyzed using a Zeiss Axioskop 2 florescence microscope with a Hamamatsu ORCA digital camera, a Zeiss LSM510 META confocal microscope, or an Olympus IX81 microscope equipped with a motorized z-stage and a Hamamatsu ORCA-ER CCD camera. For quantification, three sections per mouse, three mice per group were evaluated. Primary antibodies used were rabbit anti-α-internexin, mouse anti-proteolipid protein (PLP) and rabbit anti-Sox2 (Millipore, Temecula, CA), rabbit anti-doublecortin and rabbit anti-caspase-3, which recognizes the activated form of this protein (Cell Signaling, Danvers, MA), rabbit anti-glial fibrillary acidic protein (GFAP) and rabbit anti-myelin basic protein (MBP) (DakoCytomation, Glastrup, Denmark, UK). Cell counts for Sox2 and caspase-3 were performed in blind fashion. Five fields per section in three consecutive sections per animal were counted. Three mice per group were analyzed. Sox2 was analyzed in the subventricular area at the caudal region of the ventricle and caspase 3 in the corpus callosum. The brain structures were analyzed using hematoxylin and eosin (H&E) staining and visualized using Axiovision software on a Zeiss Axioskop CCD camera. Total cell counts were performed in a region that included the white matter and the deeper layers of the cerebral cortex, as depicted by the outlined region in Fig. 2A.

Western blot

The cerebral cortex (CX) and white matter (WM) from wild-type and CD mice were rapidly dissected and homogenized in lysis buffer containing 50 mM Tris–HCl, 0.25% sodium deoxycholate, 150 mM NaCl, 1 mM EGTA, 1% NP-40, 1 mM sodium vanadate, 1 mM AEBSF, 10 μg/ml aprotinin, 10 μg/ml leupeptin, 10 μg/ml pepstatin, and 4 μM sodium fluoride, and Western blotting analyses were performed as previously reported (Ghiani and Gallo, 2001; Ghiani et al., 2010). Protein concentrations were determined using the Pierce BCA™ Protein Assay kit (Rockford, IL). Twenty-five to 35 micrograms of total proteins were loaded onto a 4–20% Tris–glycine gel (Invitrogen, Carlsbad, CA). Equal protein loading was verified by Ponceau S solution (Sigma, Saint Louis, MI) reversible staining of the blots. Protein bands were detected by chemiluminescence using the Amersham ECL kit (GE Healthcare, Piscataway, NJ) with horseradish peroxidase-conjugated secondary antibodies (Cell Signaling, Danvers, MA). Relative intensities of the protein bands were quantified by scanning densitometry using the NIH Image Software (Image J, http://rsb.info.nih.gov/ij/). α-Tubulin was used as reference standard. The following primary antibodies were used: rabbit polyclonal anti-GFAP and rabbit polyclonal anti-MBP (DakoCytomation, Glastrup, Denmark, UK), mouse monoclonal anti-2′,3′-cyclic nucleotide 3′-phosphodiesterace (CNPase) and rabbit polyclonal anti-acetyl-histone 3 (Millipore, Temecula, CA), rabbit polyclonal anti-histone H3 (Santa Cruz Biotechnology, Santa Cruz, CA), mouse monoclonal anti-αIII tubulin (Covance, Berkeley, CA) and mouse monoclonal anti-α-tubulin (Sigma, Saint Louis, MI).

Real-time RT-PCR

Total RNA was extracted from different mouse brain areas (cerebral cortex, cerebellum, hippocampus, white matter), by using TRIzol Reagent (Invitrogen, Carlsbad, CA) as previously

reported (Ghiani et al., 2006). Six-hundred nanograms of total RNA was reverse transcribed using the iScript cDNA Synthesis Kit (BIO-RAD Laboratories, Hercules, CA). Real-time PCR was set up using the iQ SYBR® Green Supermix (BIO-RAD Laboratories, Hercules, CA), for 50 cycles, with a 30s denaturation step at 95 °C, 15s annealing step at 60 °C or 62 °C, and a 20s extension step at 72 °C. Amplification specificity was assessed by melting curve and standard curves made from serial dilutions of control RNA were used for quantification. Differences between groups were assessed by comparing ratios of our gene of interest to the gene of reference glyceraldehyde 3-phosphate dehydrogenase (GAPDH).

Primers used for real-time PCR were: ASPA (F-CATTGAGCATCCTTCACTCAAA, R-TGAGGCTGAGGACCAACTTC), nuclear factor 1 A-type (NFIA) (F-AAAGGCAAGATGCGGAGAATT, R-TGACGAGGTCCAACCTCCAT), platelet-derived growth factor receptor α (PDGFαR) (F-TCTCACTGAGATCACCACCGA, R-CGCTGTCTTCTTCCTTAGCC), CNPase (F-AACCAATGGCAGCTGTCG, R-TCAGGAACCAGCCAAAGTAAA), PLP (F-CCCACCCCTCTCCGCTAGTT, R-CAGGAAAAAAAGCACCATTGTG), myelin-associated glycoprotein (MAG) (F-GGTGTTGAGGGAGGCAGTTG, R-CGTTGTCTGCTAGGCAAGCA), ceramide-galactosyltransferase (CGT) (F-TGCCAACGTATCCTTCTTCC, R-CATTGTCCCATGTCAAGCAC) and GAPDH (F-ACTCCACTCACGGCAAATTC, R-TCTCCATGGTGGTGAAGACA).

Electron microscopy

WT and CD mice at P17, P30, 3 months and 6 months were anesthetized and perfused intracardially with 2.5% glutaraldehyde and 2% paraformaldehyde in 0.1 M cacodylate buffer pH 7.4, for 15 min at a pressure of 120 mm mercury. The brains were removed and a 1–3 mm thick section which included the corpus callosum and part of the cerebral cortex was cut. The sections were left in fixative overnight at 4 °C then washed in 0.1 M cacodylate buffer, dehydrated with graded ethanols and infiltrated with polybed/ethanol mixtures. A final infiltration step of pure Polybed 812 (Polysciences, Inc., Warrington, PA) was left overnight and subsequently oriented and embedded and left at 60 °C overnight. Sections (0.5 μm) of the specimen block were cut on a Leica Ultracut UCT microtome, stained with 1% toluidine blue in 1% sodium borate in water and the corpus callosum was then identified by light microscopy and areas were selected for ultra thin sectioning. Ultrathin sections (100 nm) were collected on copper grids, stained with 5% uranyl acetate in water, 0.4% lead citrate in 0.4% sodium hydroxide. The samples were viewed at 80 kV on a Zeiss EM910 electron microscope.

Oligodendrocyte light versus dark chromatin cell counts was performed on toluidine blue stained sections of the corpus callosum, in a blind fashion. Five fields per section, 3 sections per animal, and a minimum of 2 animals per group were evaluated.

Statistical analysis

Statistical analysis was performed using Prism 5 (GraphPad Software, San Diego, CA), by one-way ANOVA followed by Bonferrroni's multiple comparison test or Student's *t* test if only two experimental groups were compared.

Results

In the brain, neural cells develop in a highly coordinated and signal-dependent fashion. This development occurs in waves, with neurons maturing first followed by astrocytes and finally, oligodendrocytes (Qian et al., 2000; Sauvageot and Stiles, 2002). Since CD is a childhood disease, we examined the effects of ASPA deficiency on neural cells early in postnatal development.

First we analyzed the levels of ASPA expression, using real-time PCR, in the cerebral cortex and white matter of WT mice to evaluate and confirm a relationship with oligodendrocyte development. While little to no expression was seen at P1 and P7, higher ASPA expression coincided with the developmental pattern of myelin formation showing a peak between P20 and P30. Similar expression patterns were also seen in the hippocampus and the cerebellum (Fig. 1A). Gene expression levels of ASPA increased as oligodendrocytes developed and matured into a myelinating phenotype (Fig. 1B).

To understand whether ASPA deficiency affected the histoarchitecture of the brain, H&E staining was performed on brain sections of CD and WT mice from P1 until P60 (Fig. 2A). A significant increase (42%) in total cell number was detected in a region spanning from the white matter to the deeper layers of the cerebral cortex of the CD brain at P1, compared to controls (Figs. 2B and C). By P7 and P15, there was a noticeable disruption in the pattern of cell organization in CD brains. The most striking difference between CD and WT mice, however, was detected between P20 and P60, when the white matter areas of CD mice began to show an age-dependent vacuolation (Fig. 2A). Similar effects were noticed in other brain areas, such as the hippocampus and cerebellum (data not shown). With vast cytoarchitectural defects seen in CD mouse brains, which show abnormal cellular organization, we then wanted to analyze the effect of ASPA deficiency on early stages of neural cell development. Normal development of the central nervous system (CNS) and brain function is highly dependent on various transcription factors. NFIA is a transcription factor expressed in both neurons and glia cells. A lack of development of the corpus callosum due to malformation of the midline glial structures was observed in NFIA KO mice (das Neves et al., 1999;Shu et al., 2003;Plachez et al., 2008), suggesting a role for this transcription factor in normal brain development. Hence, we analyzed the expression of NFIA in the cerebral cortex of CD and WT mice by real-time PCR. The expression levels of NFIA showed a significant increase at P1 in CD mice compared to WT (Fig. 3A), while no significant differences were observed with increasing age, suggesting a possible mechanism of over compensation for the deleterious effects seen at later stages of development.

A cell count of Sox2, an early neural progenitor marker down-regulated by histone deacetylation during oligodendrocyte development (Shen et al., 2008), showed a significant decrease at P7, followed by an increase in CD mice between P15 and P30 and slightly at P60 (Figs. 3B and C). These data indicate that differentiation appears to proceed normally in CD mice until P7, but then fails and progenitor cells are present at later time points in CD mice, when neural progenitor cells are typically mostly absent.

The development of oligodendrocytes is dependent on various cell extrinsic and intrinsic signals; hence, in view of the proposed involvement of ASPA in oligodendrocyte maturation, the effect of ASPA deficiency on oligodendrocyte development was examined in an attempt to establish how early such an effect is discernable. Oligodendrocyte lineage progression from progenitors to myelinating cells in the mammalian CNS has been well characterized and markers specific for the different stages have been identified (Holz et al., 1996; Sauvageot and Stiles, 2002; Cahoy et al., 2008; Neman and deVellis, 2008). To build a developmental profile and gain a better understanding of the effect(s) of the disease on oligodendrocyte lineage progression in the CD mouse brain, some of these markers were analyzed by real-time PCR. PDGFαR, a marker for oligodendrocyte progenitors, showed no significant differences between WT and CD mice in both cerebral cortex (Fig. 4A) and white matter (data not shown), by real-time PCR. On the other hand, CNPase (Fig. 4B), a marker for immature and mature oligodendrocytes, PLP and MAG (Figs. 4C and D), both markers for mature myelinating oligodendrocytes, displayed decreased mRNA levels in CD mice cerebral cortex starting at P15, compared to WT. This decrease was statistically significant at P15, 20 and 30 for CNPase, at P15, 20, 30 and 60 for PLP and P30 for MAG (Figs. 4B–D). Similar decreases were seen in

the white matter (data not shown). CGT, an enzyme, which plays a role in myelin compaction and lipid synthesis, displayed a significant decrease at P20 in the CD cerebral cortex, with an overall trend to decrease, compared to WT (Fig. 4E). These findings demonstrate that a deficiency in the ASPA enzyme has a detrimental effect on immature, mature and myelinating oligodendrocytes, but also affects enzymes important in myelination.

The expression of oligodendrocyte genes appeared to be clearly altered in CD mice brains, thus, an ensuing effect is expected to be observed on their maturation. Acetylated histone 3 (Ac-H3) levels are inversely correlated with histone deacetylase (HDAC) activity and studies by the Casaccia-Bonnefil group (Marin-Husstege et al., 2002) have shown that HDACs 1 and 2 play a central role in oligodendrocyte development. For this reason, we asked whether loss of an enzyme affecting acetate metabolites, would also affect the levels of Ac-H3 in CD brains. In contrast to what was observed in WT animals and previously shown (Shen et al., 2008), the CD mice revealed increased, rather than decreased histone acetylation over time, with significant differences detected at P60 (Fig. 5A). The biochemical changes in post-translational modification of nucleosomal histones are best correlated with the appearance of dispersed chromatin in the nuclei. Indeed, electron microscopy (EM) revealed decreased chromatin compaction in the oligodendrocyte nuclei by P17 and up to 6 months in CD mice, compared to WT (Fig. 5B). Earlier reports had classified chromatin in oligodendrocytes as dark, medium and light, depending on the degree of compaction, with the most actively dividing cells being characterized by a light appearance of nuclei chromatin and mature oligodendrocytes by a darker chromatin (Mori and Leblond, 1970; Peters et al., 1991). Thus, the relatively low degree of chromatin compaction detected in the CD mice, is a likely indication of perturbed development and persistence of a “progenitor-like” state. This less compacted chromatin state, together with the above mentioned increase of Sox2 expression detected by P15, is suggestive of altered maturation and maintenance of the oligodendrocyte in an immature state in CD mice during late postnatal development and adulthood. An increase in the number of oligodendrocyte cells displaying non-compacted (light) chromatin and a decrease in cells with compacted (dark) chromatin was found in the corpus callosum of CD mice at all ages analyzed (Fig. 5C). These data reveal that oligodendrocyte gene expression and maturation are greatly affected by the absence of functional ASPA, however, a question still to answer is: are these cells capable of myelination? Therefore, we next investigated the levels of myelin proteins, CNPase and MBP, a major component of myelin, by Western blot. Decreased CNPase transcript levels in CD brains were seen as early as P15, with significant differences observed at P30 and P60. Decreased MBP transcripts were detected by P15, with significant decreases at P20, 30, and 60 (Fig. 6A). At the protein level, decreased MBP could be noted in CD mice as early as P15, with no differences observed at earlier time points, including P1 and P7 (Fig. 6B). The myelin marker PLP also exhibited a decreased immunoreactivity in CD mice (Supplemental Fig. 1A and B). Decreased expression of myelin gene and proteins in CD mice at P30 was also associated with a decrease in the numbers of GST-π positive cells (data not shown), which labels mature oligodendrocytes (Cammer and Zhang, 1992; Tamura et al., 2007). Because of the profound effects on myelin proteins detected in CD brains, we expected altered patterns of myelin formation. Electron microscopy analysis revealed that while in the normal brain (Fig. 6C, left panels), oligodendrocytes formed concentric myelin layers around the axons, CD brains displayed abnormally non-compact and non-concentric myelin. These findings show that CD mice exhibit severe deficits, which are all likely contributors to the pathological changes observed in this disease.

Next we analyzed the extent of cell death due to all the deficits observed in CD mice. A significantly greater number of cells positive for activated caspase-3, an apoptotic cell marker, were found in CD mice between P15 and P30, while no differences were observed at P1, P7 and P60 (Fig. 7). Double immunostaining with CNPase revealed that the majority of the caspase-3 positive cells were also CNPase positive, signifying that fewer oligodendrocytes

survive when acetylation disrupts the proper maturation process and myelin maintenance (data not shown).

Finally, we detected by Western blot a significant level of astrogliosis in CD mouse brains. The increase in GFAP was seen in CD cerebral cortex and periventricular areas as early as P15 (Figs. 8A and B), increased with age and was statistically significant at P60 (Fig. 8A). This observation was further confirmed by immunostaining. As shown in panel B of Fig. 8, the increase in GFAP in CD mice was seen by P15 and was still detectable at P60, although the staining at P60 appeared disrupted.

Discussion

Canavan disease is a devastating neurodegenerative disease characterized by a deficiency in the ASPA enzyme due to mutations, which vary among patients (Matalon et al., 1988). The lack of this enzyme leads to an accumulation of NAA and a decrease in the products acetate and aspartate derived from NAA hydrolysis, thereby affecting the acetylation state of proteins inside the cell and the synthesis of myelin-related lipids (Mehta and Namboodiri, 1995). The maturation of oligodendrocytes, the myelinating cells of the CNS, occurs mostly postnatally (Sauvageot and Stiles, 2002) and it has been correlated with the levels of acetylation on nucleosomal histones (Liu and Casaccia, 2010) that modulates gene expression and affects development. The effects of ASPA deficiency on neural cells during early postnatal development have not been analyzed. Understanding how early the cellular effects are observed may help us gain a better understanding of the disease and how it progresses in development. Consequently, since this is a disease with a childhood onset, a study which will shed light on the effects that take place early postnatally on neural cells in CD is very timely.

The scope of our work was to analyze the effects that a deficiency in ASPA enzyme activity has on early postnatal neural cell development, with a particular focus on oligodendrocytes, in order to gain a better knowledge of early pathophysiology of CD as well as disease progression. Oligodendrocyte development and myelination were studied at different postnatal ages in a mouse model which carries a mutation that affects ASPA enzyme activity (Matalon et al., 2000). Earlier reports in the tremor rat, another model for CD, suggested a possible correlation between ASPA expression and oligodendrocyte development (Bhakoo et al., 2001; Kirmani et al., 2003). In agreement with a possible role for ASPA in oligodendrocyte maturation, here we show that ASPA gene expression levels peak during myelination (P20–30) in different brain regions in WT animals. Particularly, the different regions examined displayed variations in the levels of ASPA expression, with the cerebral cortex showing the lowest. The discrepancy in the levels of ASPA among the examined regions may be due to a variety of reasons, such as the different stages of development or it could be determined by the differences in the quantity of oligodendrocytes that populate these areas. Although the cerebral cortex showed the lowest ASPA levels, we decided to focus on this region because CD individuals display vast spongy degeneration in the cerebral cortex and it is also undergoing massive developmental changes at these time points.

The expression levels of the transcription factor, NFIA were increased at P1 in CD cerebral cortex, while the neural progenitor cell marker, Sox2, was elevated late in postnatal development at P20 and P30 in CD cerebral cortex compared to WT. At the same ages, CD brains showed a noticeable decrease in the expression levels of CNPase and of the myelin genes MBP, MAG, and CGT. These effects were accompanied by a significant decline in CNPase and MBP protein levels in CD cerebral cortex, and lower MBP and PLP immunoreactivity in CD compared to WT mice. Most importantly, as shown by EM, CD brains displayed less myelin as well as the formation of uncompacted non-concentric myelin. In an attempt to further clarify how ASPA deficiency affects oligodendrocyte maturation and myelination, we

analyzed Ac-H3 levels, since it is well established that they are inversely correlated with HDAC activity and HDACs play a vital role in oligodendrocyte development and maturation (Marin-Husstege et al., 2002; He et al., 2007). The presence of increased Ac-H3 levels in CD mouse cerebral cortex suggested that oligodendrocyte maturation is hindered and fewer mature oligodendrocytes are present, compared to WT. This finding was further confirmed by the presence of a high percentage of oligodendrocyte cell nuclei with more dispersed chromatin, an indication of progenitor-like cells (Peters et al., 1991). Neuronal signaling also plays a pivotal role in oligodendrocyte maturation and myelination (Chen et al., 2010), hence, we analyzed markers for immature neurons in WT and CD mice and found that both doublecortin and α-internexin displayed an atypical expression pattern at P1 and P7, however, protein levels for β-III tubulin, another neuronal marker, showed no differences (Menezes and Luskin, 1994; Menezes et al., 1995) (Supplemental Fig. 2). These results show that neurons are formed, although appear to display an altered distribution in the CD cerebral cortex, suggesting that both oligodendrocytes and neurons are affected by ASPA deficiency. It could be speculated that ASPA deficiency affects oligodendrocyte maturation directly leading to fewer mature cells but also indirectly as a consequence of its effects on neurons. For this reason, at later postnatal stages when myelination begins, the neurons are not able to fully support oligodendrocytes and guide myelination in CD brains. The dysregulation of neuronal signaling is likely to play a role in CD pathophysiology, a finding that calls for further investigation.

Our findings show that the development of oligodendrocytes was hindered by ASPA deficiency as early as P15. Furthermore, we can infer that the temporal window between P15 and P20 appears to be a critical period for disease progression, as it is characterized by the most significant differences in oligodendrocyte and myelin gene expression between CD and WT mice. Studies have shown that the synthesis and metabolism of NAA play a role in myelination and that increased or decreased levels of this metabolite are associated with myelin abnormalities (Ledeen et al., 2006; Satrustegui et al., 2007). NAA derived acetate has been directly implicated in myelin lipid synthesis (Chakraborty and Ledeen, 2003). Although degeneration and myelin abnormalities are observed in CD mice brains, acetate diffuses from other areas of the brain and body (Ballard, 1972), thus, the partial myelination seen in this mouse model is not surprising, and suggest that lack of NAA derived acetate is unlikely to be the sole cause in CD pathophysiology. Overall, the effect on myelin in CD mice was quite extensive, and even though several cells remained in a progenitor-like state, other cells differentiated, but formed abnormal, non-compact myelin which also may contribute to disease pathology.

Many of the studies in CD animal models were performed at later stages of postnatal development (Madhavarao et al., 2005; Traka et al., 2008; Kumar et al., 2009). Here we show that development is already impaired early postnatally and our model also exhibited increased vacuolation and myelin abnormalities. Our findings are supported by previous studies in another model for CD, the tremor rat, which exhibits a spontaneous mutation (Madhavarao et al., 2005; Namboodiri et al., 2006; Wang et al., 2009). Hypomyelination, vacuolation with spongy degeneration and loss of oligodendrocytes were reported in the tremor rat model (Kondo et al., 1991; Francis et al., 2006) together with decreased lipid synthesis, suggesting that the latter could subsequently impact myelin formation (Namboodiri et al., 2006; Wang et al., 2009). In addition, our lab has shown that adult CD mice display an increased presence of progenitor cells (Kumar et al., 2009), indicating that the increase in progenitor cells seen at an early age, persists into adulthood.

Recently, another mouse model for CD was described (ENU-induced Nur7 mouse mutant), and displays a much milder phenotype (Traka et al., 2008), in contrast to the CD mouse used in this paper, which demonstrates a more severe pathology. The nur7 mouse does not show the dramatic decrease in myelin proteins we describe and the white matter seems less impacted,

as the nur7 mouse appears to be normal. These are two intrinsically different models, carrying different types of mutations, which resembles the human counterpart. In humans, CD has been shown to have a number of different mutations (Surendran et al., 2003a and depending on where the mutation is located, the severity of disease ranges from mild to severe (Traeger and Rapin, 1998; Surendran et al., 2003b). Therefore, these two mouse models can represent a mild and severe form of CD, which can both be studied to understand and identify the mechanisms underlying disease progression and gain a better comprehension of how different mutations contribute to a difference in disease pathology and its severity.

To our knowledge, this is one of the first reports to describe early postnatal defects in oligodendrocyte maturation caused by a deficiency in ASPA. In conclusion, we characterized the effect of ASPA deficiency on early postnatal developmental events and began to unravel the cellular and molecular mechanisms that contribute to CD pathophysiology. Our findings suggest that a deficiency in the ASPA enzyme affects oligodendrocyte maturation and myelination and are the first to report a defect in neuronal patterning and therefore, a possible role for these cells in triggering hypomyelination in CD. The effect of ASPA deficiency on neural cell development described in this report will enable researchers to further investigate different aspects of disease progression and develop new interventions, focused on the early events in neural cell pathology.

Supplementary Material

Refer to Web version on PubMed Central for supplementary material.

Acknowledgments

The authors are grateful to Dr. Carolyn Houser and Birgitta Sjostrand for help and advices with electron microscopy, and to Scott Fish, Teresita Yang and Jemily Malvar for technical assistance. The authors also wish to thank Dr. Esteban Dell'Angelica for insightful advice and help with fluorescent microscopy, Dr. Ellen Carpenter, Elvira Khialeeva, and Diana Anthony for their help with the H&E staining technique, Drs. Anthony Campagnoni and Pablo Paez for help with the use of the Olympus Spinning Disc Confocal Inverted Microscope. We would also like to thank Donna Crandall of the UCLA-IDDRC Media Core for help with the figures. This work was supported by grants from the NINDS-Rita L. Kirschstein NRSA Fellowship to N.S.M., a Stein-Oppenheimer Endowment Award to C.A.G. and J.d.V., NIH grants P01-HD06576, HD04612 and NMSS PP1585 to J.d.V., RO1-NS42925-08 and ARRA supplement NS42925-S1 to P.C. and the Jules Stein Core grant at UCLA-EY00331 to D.B.

References

Adachi M, Schneck L, Cara J, Volk BW. Spongy degeneration of the central nervous system (van Bogaert and Bertrand type; Canavan's disease). A review Hum Pathol 1973;4:331–347.

Ballard FJ. Supply and utilization of acetate in mammals. Am J Clin Nutr 1972;25:773–779. [PubMed: 4558368]

Baslow MH. Molecular water pumps and the aetiology of Canavan disease: a case of the sorcerer's apprentice. J Inherit Metab Dis 1999;22:99–101. [PubMed: 10234603]

Bhakoo KK, Pearce D. In vitro expression of N-acetyl aspartate by oligodendrocytes: implications for proton magnetic resonance spectroscopy signal in vivo. J Neurochem 2000;74:254–262. [PubMed: 10617127]

Bhakoo KK, Craig TJ, Styles P. Developmental and regional distribution of aspartoacylase in rat brain tissue. J Neurochem 2001;79:211–220. [PubMed: 11595773]

Bluml S. In vivo quantitation of cerebral metabolite concentrations using natural abundance 13C MRS at 1.5 T. J Magn Reson 1999;136:219–225. [PubMed: 9986765]

Burri R, Steffen C, Herschkowitz N. N-acetyl-L-aspartate is a major source of acetyl groups for lipid synthesis during rat brain development. Dev Neurosci 1991;13:403–411. [PubMed: 1809557]

Cahoy JD, Emery B, Kaushal A, Foo LC, Zamanian JL, Christopherson KS, Xing Y, Lubischer JL, Krieg PA, Krupenko SA, Thompson WJ, Barres BA. A transcriptome database for astrocytes, neurons, and

oligodendrocytes: a new resource for understanding brain development and function. J Neurosci 2008;28:264–278. [PubMed: 18171944]

Cammer W, Zhang H. Localization of Pi class glutathione-S-transferase in the forebrains of neonatal and young rats: evidence for separation of astrocytic and oligodendrocytic lineages. J Comp Neurol 1992;321:40–45. [PubMed: 1613138]

Chakraborty G, Ledeen R. Fatty acid synthesizing enzymes intrinsic to myelin. Brain Res Mol Brain Res 2003;112:46–52. [PubMed: 12670701]

Chakraborty G, Mekala P, Yahya D, Wu G, Ledeen RW. Intraneuronal N-acetylaspartate supplies acetyl groups for myelin lipid synthesis: evidence for myelin-associated aspartoacylase. J Neurochem 2001;78:736–745. [PubMed: 11520894]

Chen Z, Ma Z, Wang Y, Li Y, Lu H, Fu S, Hang Q, Lu PH. Oligodendrocyte-spinal cord explant co-culture: an in vitro model for the study of myelination. Brain Res 2010;1309:9–18. [PubMed: 19879858]

D'Adamo AF Jr, Gidez LI, Yatsu FM. Acetyl transport mechanisms. Involvement of N-acetyl aspartic acid in de novo fatty acid biosynthesis in the developing rat brain. Exp Brain Res 1968;5:267–273. [PubMed: 5712694]

das Neves L, Duchala CS, Tolentino-Silva F, Haxhiu MA, Colmenares C, Macklin WB, Campbell CE, Butz KG, Gronostajski RM. Disruption of the murine nuclear factor I-A gene (Nfia) results in perinatal lethality, hydrocephalus, and agenesis of the corpus callosum. Proc Natl Acad Sci USA 1999;96:11946–11951. [PubMed: 10518556]

de Coo IF, Gabreels FJ, Renier WO, de Pont JJ, van Haelst UJ, Veerkamp JH, Trijbels JM, Jaspar HH, Renkawek K. Canavan disease: neuromorphological and biochemical analysis of a brain biopsy specimen. Clin Neuropathol 1991;10:73–78. [PubMed: 2054980]

Francis JS, Olariu A, McPhee SW, Leone P. Novel rolefor aspartoacylasein regulation of BDNF and timing of postnatal oligodendrogenesis. J Neurosci Res 2006;84:151–169. [PubMed: 16634055]

Ghiani CA, Gallo V. Inhibition of cyclin E-cyclin-dependent kinase 2 complex formation and activity is associated with cell cycle arrest and withdrawal in oligodendrocyte progenitor cells. J Neurosci 2001;21:1274–1282. [PubMed: 11160398]

Ghiani CA, Lelievre V, Beltran-Parrazal L, Sforza DM, Malvar J, Smith DJ, Charles AC, Ferchmin PA, Vellis J. Gene expression is differentially regulated by neurotransmitters in embryonic neuronal cortical culture. J Neurochem 2006;97 (Suppl 1):35–43. [PubMed: 16635248]

Ghiani CA, Starcevic M, Rodriguez-Fernandez IA, Nazarian R, Cheli VT, Chan LN, Malvar JS, de Vellis J, Sabatti C, Dell'Angelica EC. The dysbindin-containing complex (BLOC-1) in brain: developmental regulation, interaction with SNARE proteins and role in neurite outgrowth. Mol Psychiatry 2010;15 (115):204–215.

Hagenfeldt L, Bollgren I, Venizelos N. N-acetylaspartic aciduria due to aspartoacylase deficiency–a new aetiology of childhood leukodystrophy. J Inherit Metab Dis 1987;10:135–141. [PubMed: 3116332]

He Y, Sandoval J, Casaccia-Bonnefil P. Events at the transition between cell cycle exit and oligodendrocyte progenitor differentiation: the role of HDAC and YY1. Neuron Glia Biol 2007;3:221–231. [PubMed: 18634613]

Holz A, Schaeren-Wiemers N, Schaefer C, Pott U, Colello RJ, Schwab ME. Molecular and developmental characterization of novel cDNAs of the myelin-associated/oligodendrocytic basic protein. J Neurosci 1996;16:467–477. [PubMed: 8551331]

Kaul R, Casanova J, Johnson AB, Tang P, Matalon R. Purification, characterization, and localization of aspartoacylase from bovine brain. J Neurochem 1991;56:129–135. [PubMed: 1987315]

Kirmani BF, Jacobowitz DM, Namboodiri MA. Developmental increase of aspartoacylase in oligodendrocytes parallels CNS myelination. Brain Res Dev Brain Res 2003;140:105–115.

Klugmann M, Symes CW, Klaussner BK, Leichtlein CB, Serikawa T, Young D, During MJ. Identification and distribution of aspartoacylase in the postnatal rat brain. NeuroReport 2003;14:1837–1840. [PubMed: 14534431]

Kondo A, Nagara H, Akazawa K, Tateishi J, Serikawa T, Yamada J. CNS pathology in the neurological mutant rats zitter, tremor and zitter-tremor double mutant (spontaneously epileptic rat, SER). Exaggeration of clinical and neuropathological phenotypes in SER Brain 1991;114 (Pt 2):979–999.

Kumar S, Mattan NS, de Vellis J. Canavan disease: a white matter disorder. Ment Retard Dev Disabil Res Rev 2006;12:157–165. [PubMed: 16807907]

Kumar S, Biancotti JC, Matalon R, de Vellis J. Lack of aspartoacylase activity disrupts survival and differentiation of neural progenitors and oligodendrocytes in a mouse model of Canavan disease. J Neurosci Res 2009;87:3415–3427. [PubMed: 19739253]

Ledeen RW, Wang J, Wu G, Lu ZH, Chakraborty G, Meyenhofer M, Tyring SK, Matalon R. Physiological role of N-acetylaspartate: contribution to myelinogenesis. Adv Exp Med Biol 2006;576(131–43): 361–363. discussion.

Liu J, Casaccia P. Epigenetic regulation of oligodendrocyte identity. Trends Neurosci 2010;33:193–201. [PubMed: 20227775]

Madhavarao CN, Moffett JR, Moore RA, Viola RE, Namboodiri MA, Jacobowitz DM. Immunohistochemical localization of aspartoacylase in the rat central nervous system. J Comp Neurol 2004;472:318–329. [PubMed: 15065127]

Madhavarao CN, Arun P, Moffett JR, Szucs S, Surendran S, Matalon R, Garbern J, Hristova D, Johnson A, Jiang W, Namboodiri MA. Defective N-acetylaspartate catabolism reduces brain acetate levels and myelin lipid synthesis in Canavan's disease. Proc Natl Acad Sci USA 2005;102:5221–5226. [PubMed: 15784740]

Marin-Husstege M, Muggironi M, Liu A, Casaccia-Bonnefil P. Histone deacetylase activity is necessary for oligodendrocyte lineage progression. J Neurosci 2002;22:10333–10345. [PubMed: 12451133]

Matalon R, Michals K, Sebesta D, Deanching M, Gashkoff P, Casanova J. Aspartoacylase deficiency and N-acetylaspartic aciduria in patients with Canavan disease. Am J Med Genet 1988;29:463–471. [PubMed: 3354621]

Matalon R, Kaul R, Gao GP, Michals K, Gray RG, Bennett-Briton S, Norman A, Smith M, Jakobs C. Prenatal diagnosis for Canavan disease: the use of DNA markers. J Inherit Metab Dis 1995;18:215–217. [PubMed: 7564250]

Matalon R, Rady PL, Platt KA, Skinner HB, Quast MJ, Campbell GA, Matalon K, Ceci JD, Tyring SK, Nehls M, Surendran S, Wei J, Ezell EL, Szucs S. Knock-out mouse for Canavan disease: a model for gene transfer to the central nervous system. J Gene Med 2000;2:165–175. [PubMed: 10894262]

Mehta V, Namboodiri MA. N-acetylaspartate as an acetyl source in the nervous system. Brain Res Mol Brain Res 1995;31:151–157. [PubMed: 7476023]

Menezes JR, Luskin MB. Expression of neuron-specific tubulin defines a novel population in the proliferative layers of the developing telencephalon. J Neurosci 1994;14:5399–5416. [PubMed: 8083744]

Menezes JR, Smith CM, Nelson KC, Luskin MB. The division of neuronal progenitor cells during migration in the neonatal mammalian forebrain. Mol Cell Neurosci 1995;6:496–508. [PubMed: 8742267]

Miller RH. Oligodendrocyte origins. Trends Neurosci 1996;19:92–96. [PubMed: 9054062]

Moffett JR, Ross B, Arun P, Madhavarao CN, Namboodiri AM. N-Acetylaspartate in the CNS: from neurodiagnostics to neurobiology. Prog Neurobiol 2007;81:89–131. [PubMed: 17275978]

Mori S, Leblond CP. Electron microscopic identification of three classes of oligodendrocytes and a preliminary study of their proliferative activity in the corpus callosum of young rats. J Comp Neurol 1970;139:1–28. [PubMed: 4191626]

Namboodiri AM, Moffett JR, Arun P, Mathew R, Namboodiri S, Potti A, Hershfield J, Kirmani B, Jacobowitz DM, Madhavarao CN. Defective myelin lipid synthesis as a pathogenic mechanism of Canavan disease. Adv Exp Med Biol 2006;576(145–63):361–363. discussion.

Neman, J.; deVellis, J. Handbook of neurochemistry and molecular neurobiology. Springer; US: 2008.

Peters, A.; Palay, SL.; Webster, Hd. The fine structure of the nervous system: neurons and their supporting cells. Oxford University Press; New York: 1991.

Plachez C, Lindwall C, Sunn N, Piper M, Moldrich RX, Campbell CE, Osinski JM, Gronostajski RM, Richards LJ. Nuclear factor I gene expression in the developing forebrain. J Comp Neurol 2008;508:385–401. [PubMed: 18335562]

Qian X, Shen Q, Goderie SK, He W, Capela A, Davis AA, Temple S. Timing of CNS cell generation: a programmed sequence of neuron and glial cell production from isolated murine cortical stem cells. Neuron 2000;28:69–80. [PubMed: 11086984]

Satrustegui J, Pardo B, Del Arco A. Mitochondrial transporters as novel targets for intracellular calcium signaling. Physiol Rev 2007;87:29–67. [PubMed: 17237342]

Sauvageot CM, Stiles CD. Molecular mechanisms controlling cortical gliogenesis. Curr Opin Neurobiol 2002;12:244–249. [PubMed: 12049929]

Shen S, Liu A, Li J, Wolubah C, Casaccia-Bonnefil P. Epigenetic memory loss in aging oligodendrocytes in the corpus callosum. Neurobiol Aging 2008;29:452–463. [PubMed: 17182153]

Shu T, Butz KG, Plachez C, Gronostajski RM, Richards LJ. Abnormal development of forebrain midline glia and commissural projections in Nfia knock-out mice. J Neurosci 2003;23:203–212. [PubMed: 12514217]

Surendran S, Matalon KM, Tyring SK, Matalon R. Molecular basis of Canavan's disease: from human to mouse. J Child Neurol 2003a;18:604–610. [PubMed: 14572138]

Surendran S, Michals-Matalon K, Quast MJ, Tyring SK, Wei J, Ezell EL, Matalon R. Canavan disease: a monogenic trait with complex genomic interaction. Mol Genet Metab 2003b;80:74–80. [PubMed: 14567959]

Tamura Y, Kataoka Y, Cui Y, Takamori Y, Watanabe Y, Yamada H. Intracellular translocation of glutathione S-transferase pi during oligodendrocyte differentiation in adult rat cerebral cortex in vivo. Neuroscience 2007;148:535–540. [PubMed: 17681700]

Traeger EC, Rapin I. The clinical course of Canavan disease. Pediatr Neurol 1998;18:207–212. [PubMed: 9568915]

Traka M, Wollmann RL, Cerda SR, Dugas J, Barres BA, Popko B. Nur7 is a nonsense mutation in the mouse aspartoacylase gene that causes spongy degeneration of the CNS. J Neurosci 2008;28:11537–11549. [PubMed: 18987190]

Wang J, Matalon R, Bhatia G, Wu G, Li H, Liu T, Lu ZH, Ledeen RW. Bimodal occurrence of aspartoacylase in myelin and cytosol of brain. J Neurochem 2007;101:448–457. [PubMed: 17254025]

Wang J, Leone P, Wu G, Francis JS, Li H, Jain MR, Serikawa T, Ledeen RW. Myelin lipid abnormalities in the aspartoacylase-deficient tremor rat. Neurochem Res 2009;34:138–148. [PubMed: 18478328]

Appendix A. Supplementary data

Supplementary data associated with this article can be found, in the online version, at doi: 10.1016/j.nbd.2010.07.003.

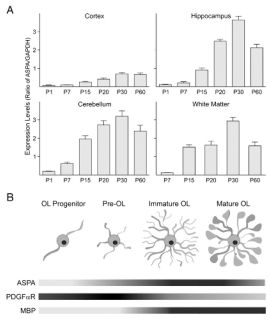

Fig. 1.

ASPA gene expression is developmentally regulated in WT mice. ASPA expression in WT mice was measured by real-time PCR in different brain areas. A modest expression is seen early in postnatal (P) development, while later ages show increased expression of ASPA, which peaks between P20 and P30. Bar graph represents the mean±SEM of 3 independent samples. B) Schematic showing the temporal relationship between oligodendrocyte maturation and ASPA gene expression. Figure modified from Neman and deVellis, 2008. Two markers involved in early (PDGFαR) and late (MBP) oligodendrocyte development show that the level of ASPA expression increases as oligodendrocytes become more mature and myelinate.

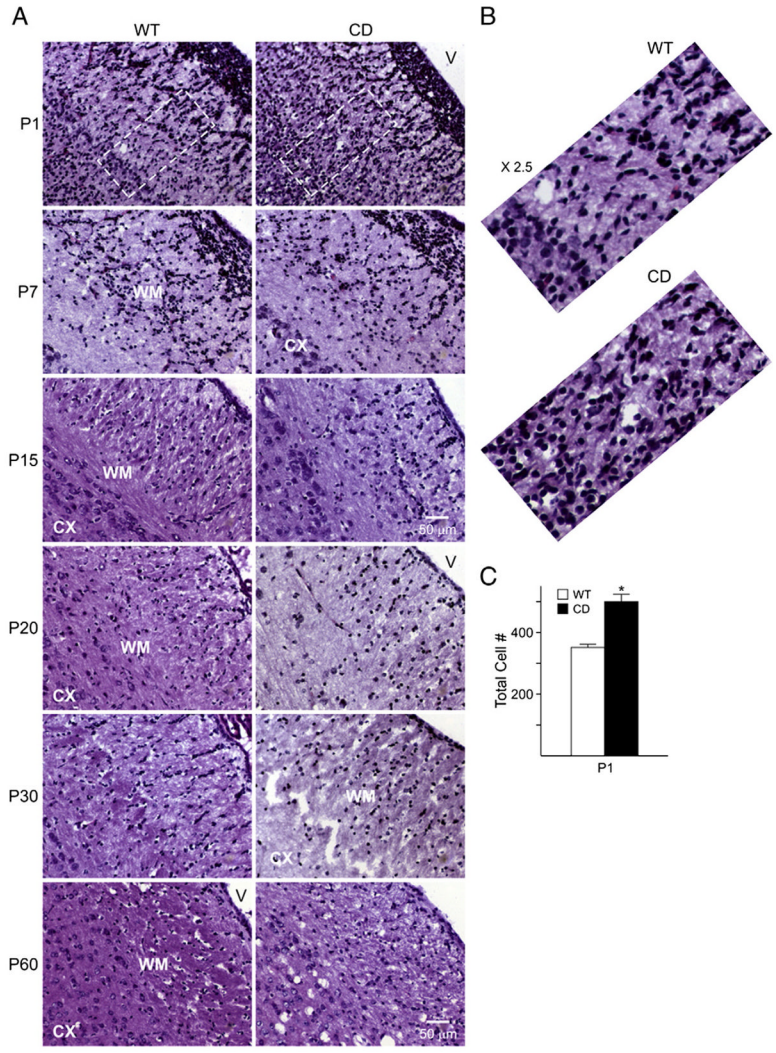

Fig. 2.

Cerebral cortex cytoarchitecture is disrupted in CD mice. A) Increased cell number is observed by H&E staining in the white matter and cerebral cortex of P1 CD mice. At later ages, a decrease in compaction along with a disorganized cell distribution and vacuolation is observed adjacent to the white matter. Less distinction between the cerebral cortex and white matter areas is seen in CD mice. B) Zoom in (×2.5) of the outlined region on P1 demonstrates an increase of cells in CD mice. C) Cell count of total cell number showing an increase in CD mice at P1. Cell counting was performed in an area that spanned from the white matter to the deeper layers of the cerebral cortex. Graph represents the mean±SEM of 3 independent animals/group. (**P*<0.05, one-way ANOVA followed by Student's *t* test). Scale bar=50 um, all the images shown in the different panels were acquired at the same magnification. Abbreviations: CX, cerebral cortex; WM, white matter; V, ventricle.

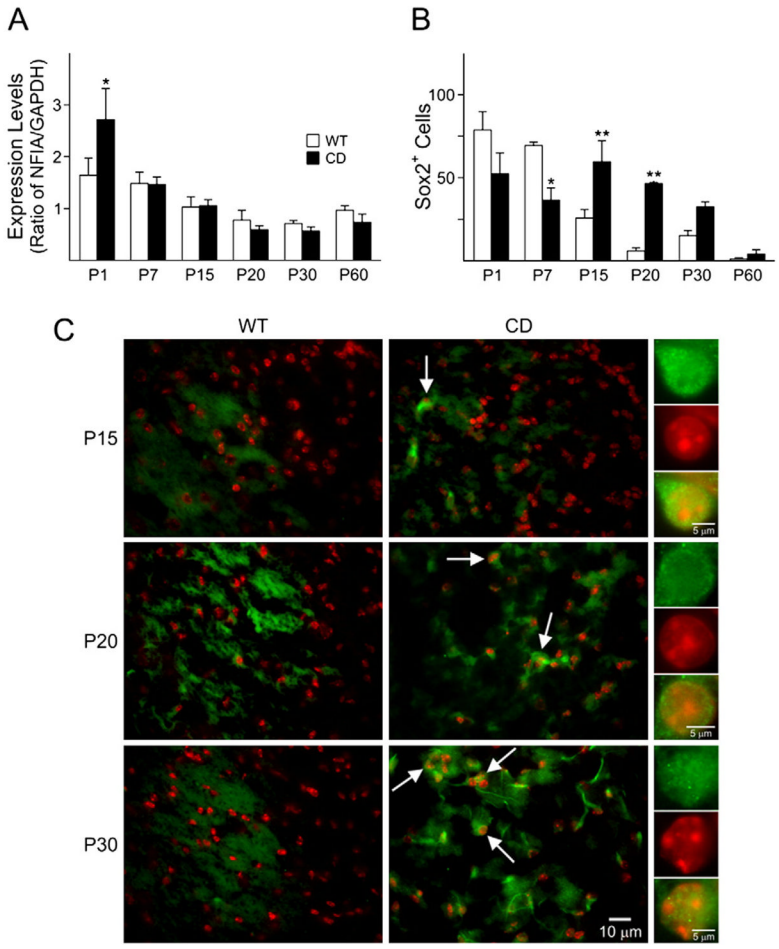

Fig. 3.

ASPA-deficient mice display an abnormal expression of neural cell markers in the cerebral cortex. A) Real-time PCR for NFIA, CD mice exhibited a significant increase in NFIA expression levels at P1, whereas later ages showed a tendency to decrease compared to WT. B) Cells counts for Sox2 positive cells decreased at P7 and increased at P15 and 20. Bar graph are the mean±SEM of 3 animals/group. (**P*<0.05; ***P*<0.01, one-way ANOVA followed by Bonferroni's multiple comparison test; WT=empty columns, CD=filled columns). C) Staining showing a significant increase in Sox2 (green) positive cells at P15, 20 and 30 (arrows). Nuclei were counterstained with To-Pro-3(red). Scale bar=10 µm. Higher magnification of a positive cell is seen in the panels on the right. Scale bar=5 µm. All the images shown in the different panels were acquired at the same magnification.

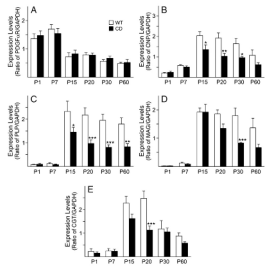

Fig. 4.

Dysregulation of oligodendrocyte gene expression in CD mouse cerebral cortex. Gene expression levels for oligodendrocyte-specific genes were measured by real-time PCR at different postnatal ages. A) Expression of PDGFαR is not significantly different in WT and CD mice. The levels of B) CNP, C) PLP, D) MAG and E) CGT expression levels are significantly decreased in CD mice as early as P15, compared to WT mice. Bar graphs are the mean±SEM of 3–4 animals/group. (**P*<0.05; ***P*<0.01; ****P*<0.001, one-way ANOVA followed by Bonferroni's multiple comparison test).

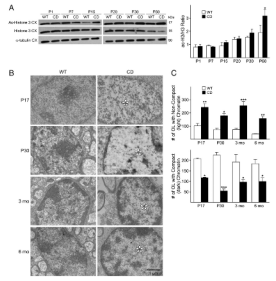

Fig. 5.

A decrease in chromatin compaction in CD mice reveals a defect in oligodendrocyte maturation. A) Representative Western blot showing that protein levels of acetylated histone 3 are increased in CD compared to WT brains by P15. No differences were observed in H3 or α-tubulin protein levels. Bar graph represents the ratio of acetylated histone 3 to histone 3, and is the mean±SEM of 3–4 animals/group. A significant increase is observed at P60 (**P*<0.05, one-way ANOVA followed by Bonferroni's multiple comparison test). B) Electron microscopy. Decreased chromatin compaction is seen as early as P17 in CD mice brains (*), WT are representative of dark chromatin and CD of light chromatin. Scale bar=1 μm. All the images were acquired using the same magnification. C) Cell counts for compact (dark) and non-compact (light) chromatin in oligodendrocytes. Bar graphs are the mean±SEM of 2 animals/group. (**P*<0.05; ***P*<0.01; ****P*<0.001, one-way ANOVA followed by Bonferroni's multiple comparison test).

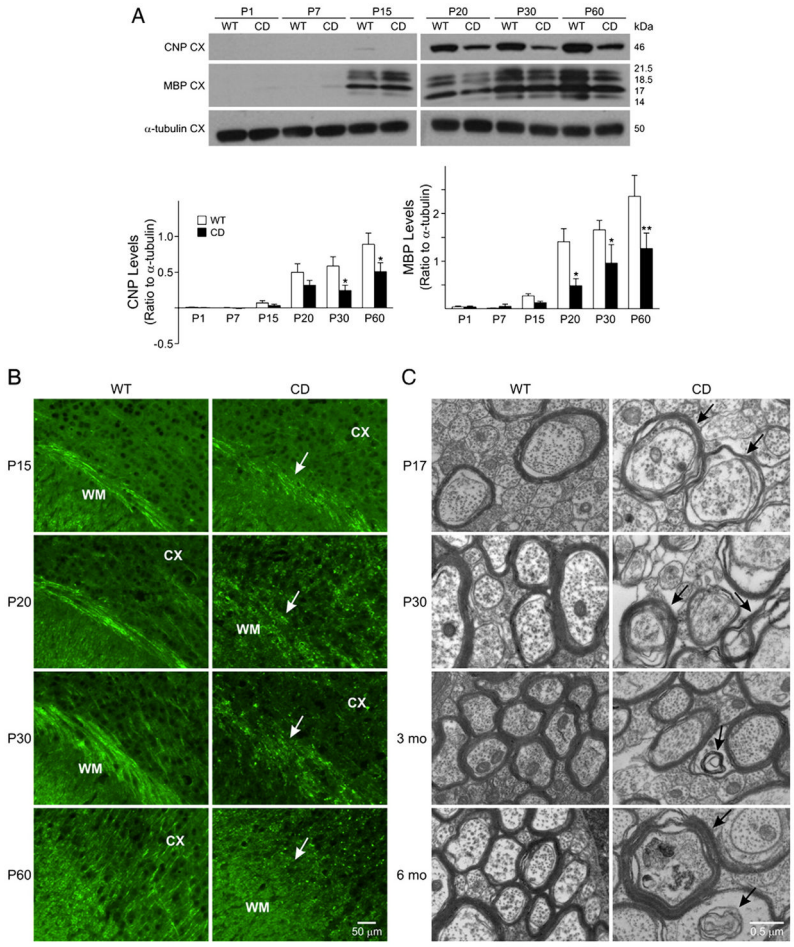

Fig. 6.

CD mice display decreased myelin protein levels and a disrupted pattern of myelination. A) Decreased CNP and MBP protein levels are seen beginning at P15. Bar graphs are the mean ±SEM of 3–4 animals/group. (**P*<0.05; ***P*<0.01, one-way ANOVA followed by Bonferroni's multiple comparison test. B) Decreased immunostaining with MBP can be seen in the white matter in CD mice (white arrows). Scale bar=50 μm. C) Electron microscopy. Non-concentric myelin forming around axons is seen as early as P17, as well as the formation of myelin in non-axonal areas, or within previously formed myelin (black arrows). Scale bar=0.5 μm, all the images were acquired using the same magnification. Abbreviations: CX, cerebral cortex; WM, white matter.

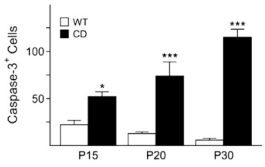

Fig. 7.

CD mice exhibit and increase in cell death. Cell counts for caspase-3 positive cells confirm an increase at P15, P20 and P30. Bar graph is the mean±SEM of 3 animals/group. (**P*<0.05; ****P*<0.001, one-way ANOVA followed by Bonferroni's multiple comparison test; WT=empty columns, CD=filled columns).

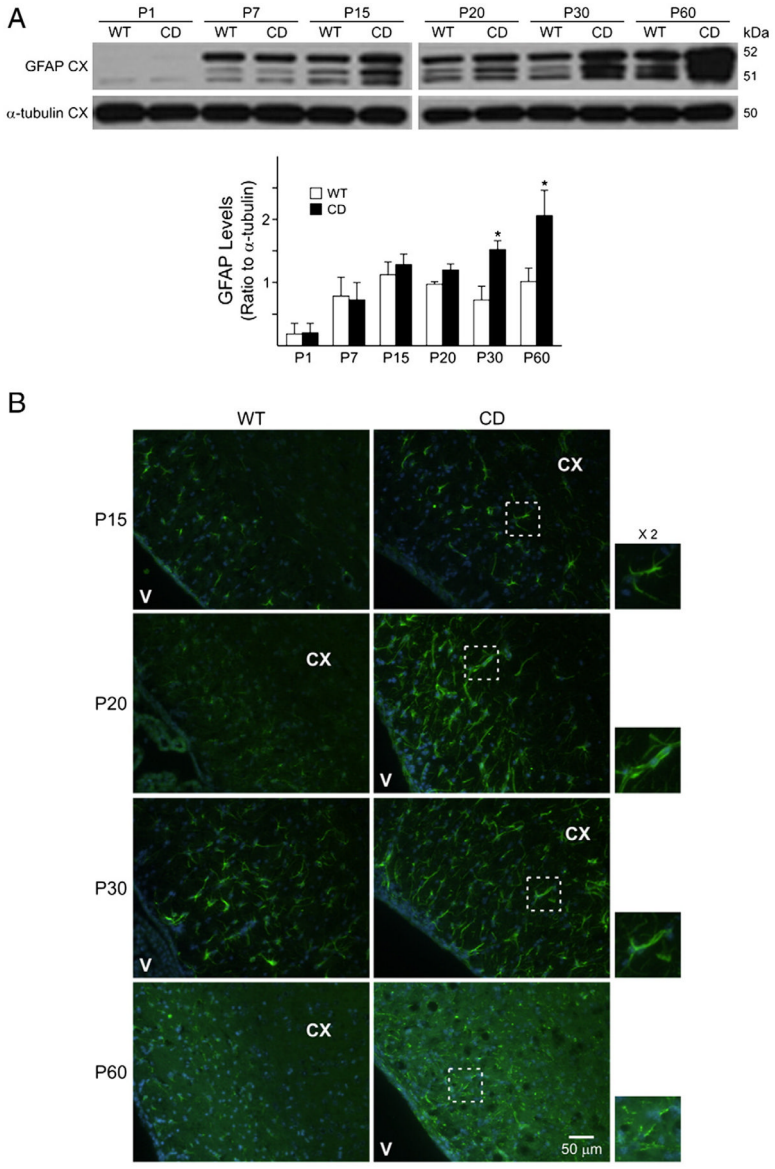

Fig. 8.

CD mice show increased expression of GFAP. A) GFAP protein levels are significantly increased in the cerebral cortex at P30 and P60. Bar graphs are the mean±SEM of 3–4 animals/group. (**P*<0.05, one-way ANOVA followed by Bonferroni's multiple comparison test). B) Hypertrophic astrocytes and increased GFAP (green) immunoreactivity is seen in CD mouse brains. Nuclei are counterstained with DAPI (blue). Scale bar=50 μm. The panels on the right show a zoom in (×2) of outlined region illustrating GFAP and DAPI. All the images were acquired using the same magnification. Abbreviations: CX, cerebral cortex; V, ventricle.